

---

# The Shapes of Random Walks

JOSEPH RUDNICK AND GEORGE GASPARI

---

**A theoretical description of the shape of a random object is presented that is analytically simple in application but quantitatively accurate. The asymmetry of the object is characterized in terms of the invariants of a tensor, analogous to the moment-of-inertia tensor, whose eigenvalues are the squares of the principal radii of gyration. The complications accompanying ensemble averaging because of random processes are greatly reduced when the object is embedded in a space of high dimensionality,  $d$ . Exact analytical expressions are presented in the case of infinite spatial dimensions, and a procedure for developing an expansion in powers of  $1/d$  is discussed for linear chain and ring-type random walks. The first two terms in such an expansion lead to results for various shape parameters that agree remarkably well with those calculated by computer simulation. The method can be extended to yield an approximate, but extremely accurate, expression for the probability distribution function directly. The theoretical approach discussed here can, in principle, be used to describe the shape of other random fractal objects as well.**

---

**T**HE SHAPE OF AN OBJECT IS ONE OF THE FIRST OF ITS properties to be noted in a casual observation. It is also one of the most important gross physical characteristics of an object. For example, the shape of an object is often a macroscopic manifestation of the microscopic principles that control its formation. The slightly aspherical shape of a planet results from and points to the balance between self-gravitational, tidal, and centrifugal forces. The shape of a crystal mirrors the regular microscopic arrangement of its constituent molecules. One observes simultaneously in the snowflake the consequences of molecular crystalline ordering and the, as yet, incompletely understood growth process that gives rise to its beautifully complex and symmetrical structure. The shapes of objects that are the result of random processes are also worthy of consideration. These shapes are a manifestation of the nature of the underlying random process, which, in addition, will influence important macroscopic properties of the object. In this article, we will outline some progress that has been achieved recently in the study of the shapes generated by a particularly simple, but important, random process. We will mention, in addition, other kinds of randomly generated objects, but the primary focus here will be the random walk.

The random walker officially arrived on the scene in a 1905 article by Pearson (*1*, p. 294): "A man starts from a point 0 and walks  $\ell$  yards in a straight line: he then turns through any angle whatever and walks another  $\ell$  yards in a second straight line. He repeats the process  $n$  times. I require the probability that after these  $n$  stretches he is at a distance between  $r$  and  $r + dr$  from the starting point 0." Since then the random walk, as a model of random processes, has been pervasive. The random walk is relevant to a wide variety of

disciplines, including the mathematics of game theory, biology, chemistry, physics, and economics (*2*). Most scientists know of the random walk because of its connection with the phenomena of Brownian motion and diffusion. Biologists have even encountered it in the meanderings of some foraging species and the migrations of certain bacteria (*3*). A variant of the random walk, the self-avoiding random walk, is important to physical chemists because it properly weights the conformations available to a chain polymer containing a large number of monomeric units whose mutual interactions occur over sufficiently short range (*4-6*); the trail left by a self-avoiding random walk can be thought of as a representation of one possible configuration of a long macromolecule. In mathematics, the random walk is recognized as the simplest example of a random fractal (*7*).

Many topics of interest to condensed matter scientists involve random fractals. Examples include percolation clusters (*8*), lattice animals (*9*), and various kinds of aggregates such as clusters of correlated spins that are characteristic of disordered magnetic systems as found in spin glasses (*10*). Since the simplest example of a random fractal is the random walk, we have chosen it as our object of study. We shall limit our discussion to some of the current notions that have proven to be amenable to analytical analysis and that appear to be useful in describing the shapes of random walks. Of course, the general concepts and the analytical approach presented in this article have direct application in characterizing the anisotropy of other random fractals as well (*11, 12*).

It is common to use averages over ensembles when discussing random walks, and, as a result, those who are not intimately familiar with the subject tend to visualize the trail left by the walker as a spherically symmetric object. However, this is not a general feature of random walks. Indeed, the trail tends to be somewhat elongated. In Fig. 1, several two-dimensional random walks, each of several thousand steps, are illustrated. The asymmetry of each is immediately evident. The fact that the path of a random walker is highly anisotropic has been known to physical chemists for some time and dates back to the early investigations of Kuhn over a half century ago (*13*). Over the years, a variety of studies exploring the shapes of random walks have appeared in the literature (*14*). In them can be found the development of useful analytical techniques and numerical algorithms to address this problem (*15*).

This article outlines a newly developed analytical approach that has yielded a number of new results and additional insights into the shapes of the trail left by a random walker. The approach presented is based on an analysis of random walks that are embedded in high spatial dimensions. Results are obtained in the form of a power series expansion in powers of one divided by dimensionality of the space in which the walk takes place, henceforth to be called a  $1/d$  expansion. A random walk in high dimension may seem far removed from the real physical situation of a walker in three spatial dimensions, but many of the predictions yielded by such an expansion,

---

J. Rudnick is professor of physics at the University of California, Los Angeles, CA 90024. G. Gaspari is professor of physics at the University of California, Santa Cruz, CA 95064.

even when truncated at very low order, especially regarding such a strongly dimensional dependent concept as shape, are remarkably accurate in three dimensions (16).

## Characterizing the Shape of a Random Walk

There are many ways to characterize the shape of an object, and no measure is both simple and complete. The quantities we will be considering describe the mean square extension of a  $d$ -dimensional object in  $d$ -orthogonal directions, one of which is the direction of the largest extent and another of which is the direction of the smallest extent. These quantities are the square of the principal radii of gyration of the object and they are the eigenvalues of a  $d \times d$  tensor,  $\mathbf{T}$ , called the radius of gyration tensor and defined by

$$T_{ij} = \frac{1}{N} \sum_{\ell=1}^N (x_{\ell i} - \langle x_i \rangle)(x_{\ell j} - \langle x_j \rangle) \quad (1)$$

where the object in question is assumed to consist of  $N$  parts, the  $\ell$ th of which is located at  $\mathbf{x}_\ell$ . The quantity  $x_{\ell i}$  is the  $i$ th component of  $\mathbf{x}_\ell$  and  $\langle x_i \rangle$  is the  $i$ th component of the mean or center of mass position

$$\langle \mathbf{x} \rangle = \frac{1}{N} \sum_{\ell=1}^N \mathbf{x}_\ell$$

Figure 2 illustrates the vectors  $\mathbf{x}_\ell$  and  $\langle \mathbf{x} \rangle$  for a two-dimensional random flight. The tensor,  $\mathbf{T}$ , is simply related to the moment-of-inertia tensor encountered in elementary classical mechanics. The gyration tensor was first introduced by Solc and Stockmeyer in their study of random flights (17). The eigenvalues of  $\mathbf{T}$  are the squares of the principal components of the radius of gyration,  $R_i^2$ ,  $1 \leq i < d$ .

The gross shape of any  $d$ -dimensional object can be obtained from appropriate ensemble averages of the eigenvalues of  $\mathbf{T}$ . If the object in question possesses the  $d$ -dimensional version of spherical symmetry, then all the  $R_i^2$  are equal. In the case of a set of randomly generated objects, the values of the  $R_i^2$ 's can be found for each member of the set, ordered by magnitude and then averaged over the set. In this way, the average intrinsic anisotropy of the object persists and is not washed away through orientational averaging. This procedure has been carried out numerically for three-dimensional unrestricted walks or walks that are not self-avoiding, and in

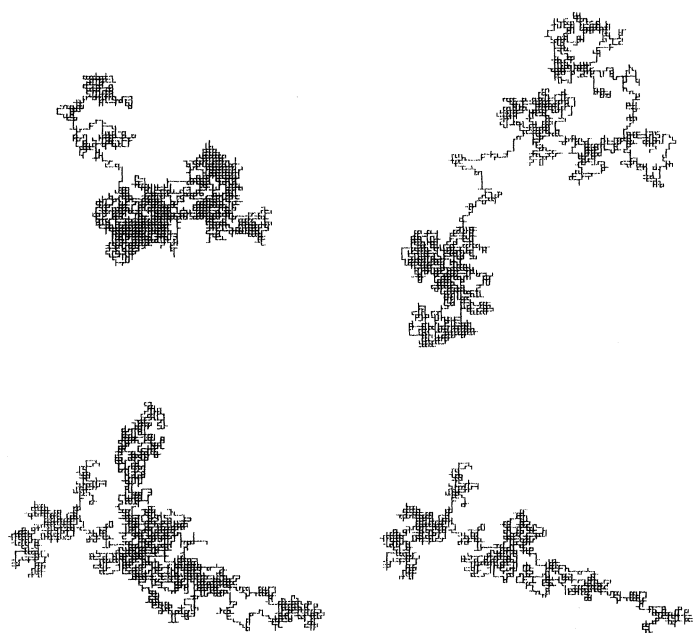


Fig. 1. Sample random walks in two dimensions of several thousand steps.

the case of long walks, the following limiting ratios have been found to be approached (18)

$$\langle R_1^2 \rangle : \langle R_2^2 \rangle : \langle R_3^2 \rangle = 11.80 : 2.69 : 1.00 \quad (2)$$

where the brackets stand for averages over many walks. Random walks are therefore far from spherical on the average. The diagonalization of a  $d \times d$  matrix is by no means a trivial task in general, but for three-dimensional walks the eigenvalues can be solved algebraically as roots to the cubic secular equation. The complicated expressions that relate the eigenvalues to the various elements of  $\mathbf{T}$  have so far resisted attempts at averaging over ensembles of random walks by analytical methods. Certain combinations of eigenvalues, however, are related in a simple and straightforward way to the invariants of  $\mathbf{T}$  and contain information regarding the average form of the random walk. The averaging process yields to analytical techniques for these quantities. For example, we have

$$R^2 = R_1^2 + R_2^2 + \cdots + R_d^2 = \text{Tr}(\mathbf{T}) = T_{11} + T_{22} + \cdots + T_{dd} \quad (3)$$

This combination of principal radii of gyration is known as the square of the radius of gyration and its average value for long, unrestricted open chain walks is the well-known results  $\langle R^2 \rangle = N/6$  (19) and for closed walks  $\langle R^2 \rangle = N/12$  (20, 21). The radius of gyration is a measure of the average extent of a random walk, however, and not its shape. A measure of the latter property is provided by the quantity  $A_d$ , called the asphericity or the asymmetry (22–24). Mathematically expressed,

$$A_d = \frac{\sum_{i>j}^d \langle (R_i^2 - R_j^2)^2 \rangle}{(d-1) \left\langle \left( \sum_{i=1}^d R_i^2 \right)^2 \right\rangle} \quad (4)$$

This quantity has zero as its lower bound, achieved for a walk that is spherical, and has an upper bound of one, a limit that is reached when the walk is extended in one dimension only. Thus,  $A_d$  is an excellent one-parameter measure of the walk's average deviation from sphericity. It can be calculated exactly for unrestricted walks, either open (23, 24) or closed (16). One finds,  $A_d = 2(d+2)/(5d+4)$  for linear chains and  $A_d = (d+2)/(5d+2)$  for walks that close on themselves. In the case of a self-avoiding walk, renormalization group calculations by Aronovitz and Nelson (24) yield the following result for  $A_d$  in  $4-\epsilon$  dimensions

$$A_d = \frac{2(d+2)}{5d+4} + 0.008\epsilon \quad (5)$$

with  $\epsilon = 1$  for three dimensions. The first term corresponds to an unrestricted walk, and the second term is the correction due to the requirement that the walk be nonintersecting. The correction factor in three dimensions is small, and somewhat larger in two dimensions

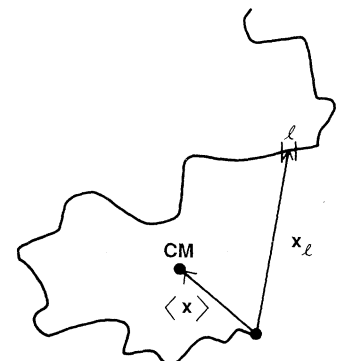


Fig. 2. The position vector of the  $\ell$ th segment of the walk,  $\mathbf{x}_\ell$ , and the mean position  $\langle \mathbf{x} \rangle$ . CM is the center of mass.

but still small, and when coupled with the fact that  $d = 4$  is the critical dimensionality in which random walks become asymptotically Gaussian (25), it is fair to say that requiring the walk to be self-avoiding has very little effect on the form of its trail for all spatial dimensionalities. Thus, as far as average shapes are concerned, the random walk can be taken to be unrestricted.

Although the quantity  $A_d$  describes the gross anisotropy of a random walk, it provides no further details concerning the shape of this object. Ideally, the most complete information would be obtained from a knowledge of the combined probability distribution function for all the principal radii of gyration, that is, a function of the form  $P(R_1^2, R_2^2, \dots, R_d^2)$ . Such a function would provide complete information on the shapes of random walks as quantified by the eigenvalues of  $\mathbf{T}$ . This distribution function in three dimensions has resisted theoretical analysis for over 50 years, but important information can be obtained to arbitrary high accuracy in high spatial dimensions. Indeed, the combined probability distribution function can, in principle, be calculated to any given order in  $1/d$ .

### Random Walks in High Spatial Dimension

The key to the analysis of high-dimensional random walks is the fact that in infinite spatial dimensionality there is essentially only one kind of walk for linear chains. Consider a walker taking a total of  $N$  steps on a hypercubic lattice that has links along the  $d$  principal axes in a Cartesian representation of the space. Each step is along a link. At the  $n$ th step, the walker can move along a direction already taken in at most  $n - 1$  ways, but there are  $(d - n + 1)$  ways of taking a step that is orthogonal to all of the previous ones. As  $d \rightarrow \infty$  the walker will with probability of one choose the latter course. All walks will consist of a set of mutually orthogonal steps. A re-ordering and, where necessary, reflection of axes maps each of them into a single walk: one in which the first step is in the positive "1" direction, the second is in the positive "2" direction, and so on.

This single dominant random walk yields a relatively simple matrix  $\mathbf{T}_\infty$  (26),

$$\begin{aligned} (T_\infty)_{ij} &= \frac{i}{(N+1)^2}(N+1-j) \text{ for } i < j \text{ and } 1 \leq i, j \leq N+1 \\ &= \frac{j}{(N+1)^2}(N+1-i) \text{ for } i > j \\ &= 0 \text{ otherwise} \end{aligned} \quad (6)$$

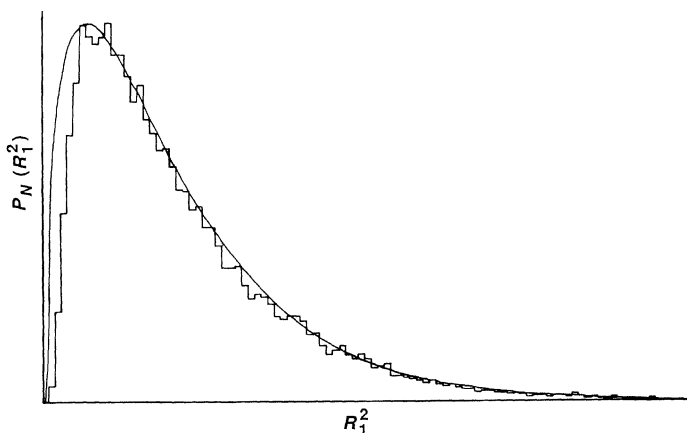


**Fig. 3.** The probability distribution,  $P_N(R_1^2)$ , of the largest principal radii of gyration,  $R_1^2$ , for  $d = 3$ . The smooth curve is the theoretical prediction given by Eq. 15. A sample of 30,000 100-step walks was used to generate the histogram.

where  $N$  is the number of steps. Its eigenvalues are, for large  $N$ ,  $R_n^2 = N/\pi^2 n^2$ . Because all walks of this type are topologically equivalent, there is no spread about these values. The distribution function  $P(R_1^2, R_2^2, \dots, R_d^2)$  is a product of delta functions. Note that the ratio of the largest to the next largest eigenvalue  $R_1^2/R_2^2 = 4$  (for  $d = \infty$ ). This is compared with the ratio from Eq. 2,  $R_1^2/R_2^2 = 4.35$ , in three dimensions. The difference between the infinite  $d$  result and the true  $d = 3$  result is slightly less than 10%. Indeed, in testing this prediction in two dimensions, a comparison with data obtained from numerical simulation by Bishop and Saltiel (27), from which one obtains  $R_1^2/R_2^2 = 5.23$ , yields an error of about 31%. The limiting ratio of the infinite dimensional random walk is preserved remarkably well down to the lowest dimension. Even closer agreement is expected by including the next order term in the  $1/d$  expansion. Careful analysis yields (26)

$$\begin{aligned} \langle R_n^2 \rangle &= \frac{N}{\pi^2 n^2} \left( 1 - \frac{1}{d} \sum_{m \neq n} \frac{n^2}{n^2 - m^2} \right) + O\left(\frac{1}{d^2}\right) \\ &= \frac{N}{\pi^2 n^2} \left( 1 + \frac{3}{4d} \right) + O\left(\frac{1}{d^2}\right) \end{aligned} \quad (7)$$

This means that the limiting ratio,  $\langle R_1^2 \rangle / \langle R_2^2 \rangle$ , is equal to 4 to within correction of order  $1/d^2$ , which accounts to some extent for the remarkable accuracy of the infinite dimensional ratios when applied to  $d = 3$ . Simulations in four and five dimensions have been carried out by Bishop and Saltiel (27). They find for a 32-step walk in five dimensions  $\langle R_1^2 \rangle = 3.95 \pm 0.17$  and  $\langle R_2^2 \rangle = 0.99 \pm 0.05$ , which implies that  $\langle R_1^2 \rangle / \langle R_2^2 \rangle = 3.99$ , a ratio that is within 1% of the order  $1/d$  prediction. In four dimensions, simulations give  $\langle R_1^2 \rangle = 4.04 \pm 0.28$  and  $\langle R_2^2 \rangle = 0.96 \pm 0.03$  so  $\langle R_1^2 \rangle / \langle R_2^2 \rangle = 4.2$  and the error is about 5%. We can do more than test ratios, however. Applying Eq. 7 to  $d = 5$ , we find that for a 32-step walk  $\langle R_1^2 \rangle = 3.74$ . The prediction thus differs from the numerical results by about 6%. In four dimensions, we predict  $\langle R_1^2 \rangle = 3.85$ , yielding a difference with the results of simulation, again of about 6%.

With the results for the eigenvalues, it now becomes feasible to apply a  $1/d$  expansion to the average of the invariants of the matrix  $\mathbf{T}$ . For example, with the aid of Eq. 7, the asphericity parameter is easily expanded to first order in  $1/d$ . One obtains

$$A_d = \frac{2}{5} + \frac{12}{25d} + O\left(\frac{1}{d^2}\right) \quad (8)$$

which yields a value of  $A_d = 0.56$  in three dimensions, whereas the exact expression gives  $A_d = 0.525$ —the error being slightly more than 6%. It should be noted that Eq. 8 can also be obtained by expanding the exact expression to order  $1/d$ . Another quantity that is similar to  $A_d$  and that also measures the walk's asymmetry but cannot be calculated exactly is

$$\langle A_d \rangle = \frac{1}{(d-1)} \left\langle \frac{\sum_{i < j} (R_i^2 - R_j^2)^2}{\left(\sum_i R_i^2\right)^2} \right\rangle \quad (9)$$

That is,  $\langle A_d \rangle$  differs from  $A_d$  in that the asphericity of each walk in the ensemble is calculated first and then the result averaged. In many ways, this quantity is the more appropriate measure of anisotropy, but, because averaging the ratio precludes the application of the techniques that were used to obtain exact results for  $A_d$ , it can only be evaluated by numerical means. Bishop and Michels have recently computed  $\langle A_d \rangle$  numerically (28) and these calculations can be compared to the results of a  $1/d$  expansion. To the two lowest orders (16),

$$\langle A_d \rangle = \frac{2}{5} - \frac{12}{175d} + O\left(\frac{1}{d^2}\right) \quad (10)$$

so that

$$\langle A_3 \rangle = 0.377 + O\left(\frac{1}{d^2}\right)$$

Simulations yield  $\langle A_3 \rangle = 0.39 \pm 0.004$ ; thus, the percentage error in the  $1/d$  expansion is, once more, of order 5 to 6%.

## The Probability Distribution Function

The information that can be gained from the  $1/d$  formalism is not restricted to averages. One can extract full information regarding the probability distribution of the principal components of the radius of gyration, order by order in  $1/d$ , from a consideration of the imaginary part of the resolvent function (29)

$$R(\lambda) = \text{Tr}\left(\frac{1}{\lambda \mathbf{I} - \mathbf{T}}\right) \quad (11)$$

where  $\lambda$  is a complex scalar constant and  $\mathbf{I}$  is the unit matrix. A class of terms contributing to all orders in  $1/d$  (in fact, the equivalent of selective summation to all orders in perturbation theory) yields the following result for the probability distribution (16),

$$P(R_1^2, R_2^2, \dots, R_N^2) = \prod_n P_N(R_n^2) \quad (12)$$

where

$$P_N(R_n^2) = \int_{-\infty}^{\infty} e^{isR_n^2} \left(1 - \frac{2iN}{d\pi n^2}\right)^{-d/2} ds$$

From this result, one immediately obtains the distribution function governing the square of the radius of gyration itself,  $R^2 = R_1^2 + R_2^2 + \dots + R_N^2$ . We have

$$P(R^2) = \int P(R_1^2, R_2^2, \dots, R_N^2) \delta(R^2 - R_1^2 - R_2^2 - \dots - R_N^2) \times dR_1^2 dR_2^2 \dots dR_N^2 \quad (13)$$

where  $\delta$  is the Dirac delta function. With the integral representation of the delta function and Eq. 12,  $P(R^2)$  becomes

$$P(R^2) = \frac{1}{2\pi} \int e^{isR^2} K(s) ds \quad (14)$$

with

$$K(s) = \prod_{n=1}^N \left(1 - \frac{2isN}{d\pi n^2}\right)^{-d/2}$$

This result (Eq. 14) for the probability distribution function for the radius of gyration itself is an exact formula first derived by Fixman (30). It is gratifying that our approximate expression for  $P(R_1^2, R_2^2, \dots, R_N^2)$  leads to an exact expression for  $P(R^2)$ .

The distribution function for the individual principal components represents a considerable success of the  $1/d$  formalism. The distribution function for the individual principal components can also be compared with numerical simulations. Figure 3 compares the distribution of the largest principal component of  $R^2$ , obtained by generating 30,000 samples of 100-step walks in  $d = 3$  dimensions, with  $P_N(R_n^2)$  derived from Eq. 12 by steepest descents integration, which is asymptotically accurate in the large  $d$  limit. We find

$$P_N(R_n^2) \propto \left(\frac{R_n^2}{\langle R_n^2 \rangle}\right)^{d-1} \exp\left(-\frac{d}{2} \frac{R_n^2}{\langle R_n^2 \rangle}\right) \quad (15)$$

where  $\langle R_n^2 \rangle = N/\pi^2 n^2$ . Note that the average  $\langle R_n^2 \rangle$  for this distribu-

tion is the zero order result whereas the variance of the distribution

$$\Delta R_n^2 = \langle (R_n^2)^2 \rangle - \langle R_n^2 \rangle^2 = \frac{2}{d} \langle R_n^2 \rangle^2 = \frac{2}{d} \frac{N^2}{\pi^4 n^4} \quad (16)$$

is exactly the first-order (in  $1/d$ ) result obtained by considering high dimensional walks directly, as described in the previous section. In Fig. 3, the predicted curve was obtained from Eq. 15, with the constant of proportionality determined to match the peak value of the numerical result. Overall, the fit is remarkably good. The discrepancy between the theoretical and the numerical distributions at small  $R_1^2$  is not a reflection of shortcomings of the theory. The counting procedure used to generate the histogram does not discriminate between eigenvalues. Thus, for finite  $d$ , eigenvalues of the ensemble with values greater than  $R_1^2$  are included in the numerical result whereas the theoretical curve is the distribution of  $R_1^2$  alone. In a strict sense, the distributions are similar but different. They both are asymptotically exact for large  $R_1^2$  but differ at small  $R_1^2$ . It is a straightforward calculation to include in the distribution the contribution of other eigenvalues, and when this is done the agreement between the theoretical predictions and the results of simulations is greatly improved (Fig. 4).

A more direct, if less comprehensive, comparison can be made between the variances of the numerical distribution and that predicted by the  $1/d$  expansion. For a 100-step walk in  $d = 3$  dimensions, Eq. 16 gives  $\Delta R_n^2/N^2 = 6.8 \times 10^{-3}$  while the simulation results have  $\Delta R_n^2/N^2 = 6.13 \times 10^{-3}$  for a percentage difference of about 11%. The agreement is encouraging and it appears that the  $1/d$  formalism works well, but additional numerical studies are needed before we can fully understand its limitations (31).

## The Shapes of Other Random Fractals

Random walks are not the only randomly generated fractals whose shapes can be studied with a  $1/d$  expansion. A variation of the open or chainlike random walk, the "ring," or self-closing walk, can also be analyzed in high dimension. It is not immediately apparent that the simplification of a single walk dominating all others in infinite dimension is correct for self-closing walks. This is because the self-closing walk can be broken up, in high dimensions, into steps "out" and steps "back." Each of the out steps is in a direction that is orthogonal to all the other out steps and the same holds for the back steps, each of which is in the opposite direction to an out

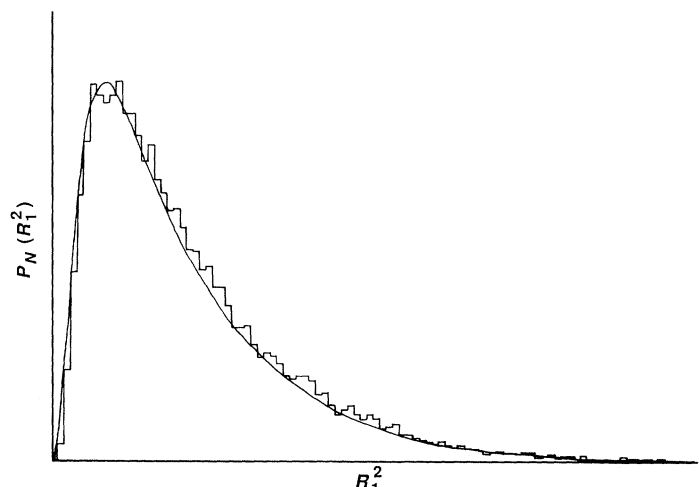


**Fig. 4.** The theoretical probability distribution in Fig. 3 is modified to include contributions from the second largest principal radii of gyration,  $R_2^2$ . The histogram, which includes these contributions, is the same as that drawn in Fig. 3.

step. However, the shape of the ring is dependent on the order of the back steps, which is arbitrary. Indeed, the walker can step out and back in a given direction before stepping out in another one. One finds statistically, though, that rings in high dimensions are almost all of the same shape, as parameterized in terms of the individual principal radii  $R_n^2$  (16). In infinite dimension, as in the case of open chain walks, the problem has an exact solution. For rings in infinite dimension, the principal radii of gyration are doubly degenerate and one-fourth the value of their chain counterparts.

$$\langle R_n^2 \rangle = \frac{1}{4} \frac{N}{\pi^2 n^2} \quad (\text{twofold degenerate}), \quad 1 \leq n \leq \frac{N+1}{2} \quad (17)$$

$$= 0 \quad \text{otherwise}$$

The asymptotic ratios of the three largest  $R_n^2$  are  $\langle R_1^2 \rangle : \langle R_2^2 \rangle : \langle R_3^2 \rangle = 4 : 4 : 1$ . One sees that in very high dimension rings become “oblate” whereas chain walks retain their “prolateness.” The double degeneracy of  $\langle R_n^2 \rangle$  for  $d = \infty$  leads to some difficulties in the development of a  $1/d$  expansion, but one can nevertheless obtain some useful results. For example, the average principal components, to order  $1/d$ , are

$$\langle R_n^2 \rangle = \frac{N}{4\pi^2 n^2} \left( 1 + \frac{3}{2d} \right) + O\left(\frac{1}{d^2}\right) \quad (18)$$

with a variance

$$\Delta R_n^2 = \left( \frac{N}{4\pi^2 n^2} \right)^2 \frac{3}{d}$$

As we mentioned earlier, the asphericity can be calculated exactly for rings,  $A_d = (d+2)/(5d+2)$  and the  $1/d$  series becomes

$$A_d = \frac{1}{5} + \frac{8}{25d} + O\left(\frac{1}{d^2}\right) \quad (19)$$

which differs from the exact expression by 3.5%. The average fluctuation in  $A_d$ , as measured by the quantity  $\langle A_d \rangle$ , cannot be calculated exactly but can be expressed as a  $1/d$  expansion,

$$\langle A_d \rangle = \frac{1}{5} + \frac{32}{175d} + O\left(\frac{1}{d^2}\right)$$

$$= 0.261 \quad (d=3) \quad (20)$$

The above prediction is to be compared with the numerical result  $\langle A_d \rangle = 0.258 \pm 0.007$  obtained from simulations by Bishop and Michels (28). The lowest order terms in the  $1/d$  series represent the various average shape parameters for rings quite well down to low dimensions. The accuracy is comparable to what was found for chains. Unfortunately, so far we have not been able to derive a satisfactory distribution function for self-closing walks, however, because of ambiguities arising from the double degeneracy.

## Conclusions

The investigation of the shapes in high dimensionality of at least two kinds of randomly generated objects thus leads to useful—and surprisingly accurate—predictions for the shapes of these objects in physical dimensionalities. An interesting question is whether the  $1/d$  formalism can be successfully applied to the study of shapes of other randomly generated clusters as well. The question remains open at the moment, but Aronovitz and Stephen (12) have recently adopted the principal radii of gyration characterization of shapes to analyze the average anisotropy of percolation clusters and lattice animals. In

particular, using renormalization group techniques, they have calculated the asymmetry parameters  $A_d$  to first order in an interdimensional expansion. They find

$$A_d = \frac{2+d}{2+6d} + \frac{607}{4410} \frac{d(d+2)}{(1+3d)^2} \epsilon_{\text{percolation}}$$

$$= \frac{2+d}{2+6d} + \frac{29}{288} \frac{d(d+2)}{(1+3d)^2} \epsilon_{\text{animal}} \quad (21)$$

where  $\epsilon_{\text{percolation}} = 6 - d$  and  $\epsilon_{\text{animal}} = 8 - d$ . From these results, it is seen that, in three dimensions, both kinds of clusters are anisotropic but less so than random walks. Lattice animals are a bit more anisotropic than percolation clusters. Whether it is possible to go beyond this gross description of the shapes of these clusters and develop a theory of the probability distribution of shapes, similar to what has been done for random walks, is an open question. If this program is indeed feasible, then the anisotropy of these random objects will be more completely specified and we can begin to develop a quantitative theory of the effects of shape on the physical properties of systems that they represent.

A guide to theoretical endeavors is provided by some recent numerical investigations. Straley and Stephen (32) have calculated various anisotropy parameters for percolation clusters in two and three dimension, and Quandt and Young (33) have evaluated the asphericity and its distribution for both percolation clusters and Ising spin clusters in two dimension. In both cases, the agreement between the numerical results and the  $\epsilon$ -expansion prediction of Aronovitz and Stephen (12) is quite good. Also, Bishop and Saltiel (34) have computed shapes and shape distribution for open and closed random walks in two, four, and five dimensions. When comparison with results of  $1/d$  expansion can be made, the agreement is also quite good.

We are encouraged by the progress made in developing analytical approaches useful to the study of random fractal objects. Renormalization group methods and the  $1/d$  expansion have led to a greatly increased ability to characterize the anisotropy of mathematical objects of interest to physical scientists, and we expect significant progress to be made in this field in the near future.

## REFERENCES AND NOTES

1. K. Pearson, *Nature (London)* **27**, 239 (1905).
2. E. W. Montroll and M. F. Shlesinger, *Nonequilibrium Phenomena II from Stochastics to Hydrodynamics*, J. L. Lebowitz and E. W. Montroll, Eds. (Elsevier, Amsterdam, 1984); also see S. Chandrasekhar, *Rev. Mod. Phys.* **15**, 1 (1943).
3. G. W. Weiss and R. J. Rubin, Eds., *J. Stat. Phys.* **30**, 2 (1983); special issue on random walks in the physical and biological sciences.
4. P. J. Flory, *Statistics of Chain Molecules* (Interscience, New York, 1969).
5. C. Domb, *Adv. Chem. Phys.* **18**, 229 (1969).
6. P.-G. de Gennes, *Scaling Concepts in Polymer Physics* (Cornell Univ. Press, Ithaca, NY, 1979) and references therein.
7. B. B. Mandelbrot, *The Fractal Geometry of Nature* (Freeman, New York, 1983).
8. As an example of a percolation cluster, consider a lattice whose sites may either be occupied or unoccupied with a specified probability. Then, for any given configuration, the occupied sites of the lattice will form clusters whose members can be connected by nearest neighbor distances; for an excellent discussion of percolation theory, see J. W. Essam, in *Phase Transitions and Critical Phenomena*, C. Domb and M. S. Green, Eds. (Academic Press, London, 1972), vol. 2, pp. 197–269.
9. A lattice animal is defined as a percolation cluster with  $t$  unoccupied boundary sites that are nearest neighbors to the occupied sites of the cluster. A good review of percolation clusters and lattice animals can be found in D. Stauffer, *Phys. Rep.* **54**, 1 (1979).
10. See for instance: T. A. Witten and M. E. Cates, *Science* **232**, 1607 (1986); F. Family and D. P. Landau, Eds., *Kinetics of Aggregation and Gelation* (Elsevier/North-Holland, Amsterdam, 1984).
11. F. Family, T. Vicsek, P. Meakin, *Phys. Rev. Lett.* **55**, 641 (1985).
12. J. Aronovitz and M. J. Stephen, in preparation.
13. W. Kuhn, *Kolloid-Zeitschrift* **68**, 2 (1934).
14. For an excellent introductory discussion of general theoretical notions regarding the shapes of polymers and a review of earlier work, see K. Solc, *Polym. News* **4**, 67 (1977).
15. P. J. Flory, *Principles of Polymer Chemistry* (Cornell Univ. Press, Ithaca, NY, 1953).

16. G. Gaspari, J. Rudnick, A. Beldjenna, *J. Phys. A*, in press.  
 17. K. Solc and H. Stockmeyer, *J. Chem. Phys.* **54**, 2756 (1971); K. Solc, *ibid.* **55**, 335 (1971).  
 18. K. Solc, *Macromolecules* **6**, 378 (1973).  
 19. P. Debye, *J. Chem. Phys.* **14**, 636 (1946).  
 20. H. A. Kramers, *ibid.*, p. 415 (1946).  
 21. B. Zimm and W. H. Stockmeyer, *ibid.* **17**, 1301 (1949).  
 22. D. N. Theodorou and U. W. Suter, *Macromolecules* **18**, 1206 (1985).  
 23. J. Rudnick and G. Gaspari, *J. Phys. A* **19**, L191 (1986).  
 24. J. Aronovitz and D. R. Nelson, *J. Phys. (Paris)* **47**, 1445 (1986).  
 25. V. Ginzburg, *Sov. Phys.-Solid State* **2**, 1824 (1960); E. Helfand and J. S. Langer, *Phys. Rev.* **160**, 427 (1967).  
 26. J. Rudnick, A. Beldjenna, G. Gaspari, *J. Phys. A* **20**, 971 (1987).  
 27. M. Bishop and C. Saliel, *J. Chem. Phys.* **85**, 6728 (1986).  
 28. M. Bishop and J. P. J. Michels, *ibid.*, p. 1074.  
 29. A. Messiah, *Quantum Mechanics* (Wiley, New York, 1968), vol. 1.  
 30. M. Fixman, *J. Chem. Phys.* **36**, 306 (1962).  
 31. The theoretical predictions based on Eq. 15 overestimate the number of walks in the region near the origin. As  $R_1^2 \rightarrow 0$ , the walks become extremely compact and the probability of finding such walks drops off abruptly. We are grateful to M. Nauenberg for helpful discussion on this point and for providing us with the results of his numerical simulations.  
 32. J. Straley and M. J. Stephen, *J. Phys. A*, in press.  
 33. S. Quandt and A. P. Young, *ibid.*, in press.  
 34. M. Bishop and C. Saliel, in preparation.  
 35. We acknowledge useful discussions with A. Beldjenna, M. Bishop, M. Nauenberg, V. Privman, and A. P. Young. We thank J. Aronovitz, D. R. Nelson, M. J. Stephen, and J. Straley for sending reports of their work prior to publication.

## Research Articles

# The 30-Kilodalton Gene Product of Tobacco Mosaic Virus Potentiates Virus Movement

CARL M. DEOM, MELVIN J. OLIVER, ROGER N. BEACHY

The proposed role of the 30-kilodalton (kD) protein of tobacco mosaic virus is to facilitate cell-to-cell spread of the virus during infection. To directly define the function of the protein, a chimeric gene containing a cloned complementary DNA of the 30-kD protein gene was introduced into tobacco cells via a Ti plasmid-mediated transformation system of *Agrobacterium tumefaciens*. Transgenic plants regenerated from transformed tobacco cells expressed the 30-kD protein messenger RNA and accumulated 30-kD protein. Seedlings expressing the 30-kD protein gene complemented the Ls1 mutant of TMV, a mutant that is temperature-sensitive in cell-to-cell movement. In addition, enhanced movement of the Ls1 virus at the permissive temperature was detected in seedlings that express the 30-kD protein gene. These results conclusively demonstrate that the 30-kD protein of tobacco mosaic virus potentiates the movement of the virus from cell to cell.

THE INITIAL ENTRY AND REPLICATION OF A PLANT VIRUS IN a susceptible host is followed by movement of progeny virus into adjacent healthy cells, a process that is necessary for spread of the infection. In many virus-host interactions, movement (transport) also includes the systemic spread of the virus (that is, into other leaves) via the conductive tissues. In contrast, in nonhost plants the virus either fails to replicate or replicates in initially infected cells but fails to move to neighboring cells. If the virus replicates but fails to spread the plant remains healthy with only the few initially infected cells containing viral progeny (1). Effectively, the infection is aborted, and the plant reacts as if resistant to the virus.

Little is known about how plant viruses move in their hosts, either cell-to-cell or systemically. However, in recent years evidence has accumulated which suggests that a specific virus-encoded product is involved in the movement process. Such a virus-encoded

function could be instrumental in determining the host range of the virus (2, 3), and within a given virus-host interaction it may be an important factor in determining virulence. In the case of tobacco mosaic virus (TMV) it has been suggested that the virus-encoded 30-kD protein is responsible for the movement function.

The genome of TMV is a single-stranded RNA of positive polarity encapsidated by a single type of capsid protein. The complete nucleotide sequence of the U<sub>1</sub> (common) strain has been determined (4), and shown to encode at least four proteins. Translation of the genomic RNA in vitro directs the synthesis of the 126-kD and 183-kD proteins. The 183-kD protein is a readthrough product of the amber termination codon of the 126-kD protein. Both proteins are postulated to be subunits of the TMV replicase (5, 6), and have been identified in virus-infected cells (7). Translation of two other open reading frames to produce the 30-kD and coat proteins requires the formation of two subgenomic RNA's, the 30-kD protein messenger RNA (mRNA), designated I<sub>2</sub> RNA (8), and the coat protein mRNA (6, 9).

Evidence implicating the 30-kD protein of TMV in movement comes from studies with temperature-sensitive (ts) mutants of TMV that are defective in cell-to-cell movement (10, 11). One well-characterized ts mutant is the Ls1 strain of TMV, a spontaneous mutant of the tomato strain L. At nonpermissive temperatures, the Ls1 strain replicates and assembles normally in inoculated leaves and in leaf protoplasts, but is not capable of moving from cell to cell in inoculated leaves (10, 12). When two-dimensional peptide mapping analysis was used to compare the 30-kD proteins encoded by I<sub>2</sub> RNA's obtained from Ls1 and L virus preparations, only a minor difference was detected (13). A comparison of the nucleotide sequences of the L and the Ls1 strains revealed that the Ls1 virus had a single base change in the 30-kD protein gene which substituted a serine for a proline residue (14). Using the Ls1 mutant,

C. M. Deom is a postdoctoral associate and R. N. Beachy is a professor in the Department of Biology, Washington University, St. Louis, MO 63130. M. J. Oliver is an assistant professor in the Department of Biology and PGEL, New Mexico State University, Las Cruces, NM 88003.